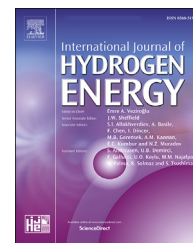




ELSEVIER

Available online at www.sciencedirect.com

ScienceDirect

journal homepage: www.elsevier.com/locate/he

Surface roughness improvement of Hastelloy X tubular filters for H₂ selective supported Pd–Ag alloy membranes preparation

S. Agnolin ^a, J. Melendez ^b, L. Di Felice ^a, F. Gallucci ^{a,c,*}

^a Inorganic Membranes and Membrane Reactors, Sustainable Process Engineering, Department of Chemical Engineering and Chemistry, Eindhoven University of Technology, De Rondom 70, Eindhoven, 5612 AP, the Netherlands

^b H₂Site, Bilbao, Spain

^c Eindhoven Institute for Renewable Energy Systems (EIRES), Eindhoven University of Technology, PO Box 513, Eindhoven, 5600 MB, the Netherlands

HIGHLIGHTS

- The surface characteristics of rough tubes have been tuned to a media grade that allows membrane deposition.
- The polishing time was assessed by studying the average support's roughness. 6 h are enough to produce good supports.
- Boehmite-based interdiffusion layers are used to change the surface quality and as interdiffusion barrier.
- Thin Pd–Ag layers can be deposited on the modified supports.

ARTICLE INFO

Article history:

Received 27 April 2022

Received in revised form

16 June 2022

Accepted 18 June 2022

Available online 16 July 2022

Keywords:

Surface modification

Metallic membranes

Hydrogen separation

Pd membranes

Metallic supports

ABSTRACT

Thin Pd–Ag layers have been successfully deposited on ceramic supports with controlled surface characteristics. The need for less fragile membranes and ease of sealing and connection leads to the study of metallic supports for thin Pd-based membrane development. Metallic supported membranes are prone to intermetallic diffusion issues so an interdiffusion barrier must be introduced. However, metallic supports with sufficient surface quality for direct membrane deposition are expensive and not readily available in the market. It is thus important to study how to improve surface roughness of commercially available rough metallic filters, in order to allow deposition of a smooth, delamination-free Pd–Ag layer.

This work reports a first attempt towards a standardized preparation procedure for Pd-based membranes on cheap, rough, and unrefined Hastelloy X tubular filters. The focus is on surface roughness reduction, in order to allow the deposition of a smooth, uniform Pd–Ag selective layer. The surface roughness of the tubes is tuned via 1) polishing and 2) addition of a smoothening interdiffusion barrier layer based on a boehmite dip-coated dispersion. The polishing time was assessed by studying the average support's roughness variation, permeation behavior and ability to retain ceramic coating. It was found that the best trade-off between polishing extent and gas permeance of the support amounts to 6 h. Moreover, it was assessed that increasing the boehmite load in the interdiffusion barrier precursor solution leads to thicker layers and larger surface roughness reduction, but greater solution instability. 1,2%wt of boehmite load proved the best trade-off between

* Corresponding author. Inorganic Membranes and Membrane Reactors, Sustainable Process Engineering, Department of Chemical Engineering and Chemistry, Eindhoven University of Technology, De Rondom 70, Eindhoven, 5612 AP, the Netherlands.

E-mail address: f.gallucci@tue.nl (F. Gallucci).

<https://doi.org/10.1016/j.ijhydene.2022.06.164>

0360-3199/© 2022 The Author(s). Published by Elsevier Ltd on behalf of Hydrogen Energy Publications LLC. This is an open access article under the CC BY license (<http://creativecommons.org/licenses/by/4.0/>).

layer reproducibility and support coverage. Different dipping-sintering routes were evaluated in order to improve surface's suitability for electroless plating: a single interdiffusion layer deposition route proved the most suitable for Pd–Ag deposition. The electroless plating performed onto the treated supports results in a continuous Pd–Ag layer, proving Pd–Ag deposition possible on the selected filters.

© 2022 The Author(s). Published by Elsevier Ltd on behalf of Hydrogen Energy Publications LLC. This is an open access article under the CC BY license (<http://creativecommons.org/licenses/by/4.0/>).

Introduction

Steam methane reforming is a widely used process to convert CH_4 into an H_2 stream. The reforming process is followed by a water gas shift reaction, which is carried out in two different units, and by further separation and purification stages. This great number of steps can be reduced with process intensification means by introducing new reactor concepts and increasing overall process efficiency. Membrane reactors (MR) are a promising technology for intensification of methane steam reforming [1,2]. Pd–Ag alloy membranes have been studied as suitable candidates for this application and other hydrogen separation implementations thanks to their unique solution-diffusion transport mechanism, leading to an outstandingly high selectivity towards H_2 [3–5]. Moreover, introducing Pd membranes in a catalytic reactor for reforming has proved to reduce operating temperatures and to increase energy efficiency by decreasing the number of process units [6–8]. Pd membranes have been subjected to optimization studies in terms of selective Pd–Ag layer thickness. The goal is to produce highly selective supported membranes and reducing the amount of used Pd at the same time. Furthermore, tubular membrane configurations have been developed for suitable integration in the reactor system [9,10]. Thin Pd–Ag layers have been successfully deposited on ceramic supports with controlled surface roughness, morphology and average pore size [11,12]. Ceramic supports are in fact suitable for Pd–Ag deposition thanks to their fine-tuned superficial characteristics (Table 3). However, their inherent low mechanical stability, the required sealing of the membrane structure, and the integration into the reactor system are the main unresolved challenges for these membranes [13,14]. The need for less fragile membranes and ease of sealing and integration into the reactor system leads to the study of suitable metallic supports. However, the deposition of a thin, defect-free Pd–Ag layer on metallic supports proves more difficult due to their poor surface quality compared to their ceramic relatives (Table 3) [15]. Furthermore, the stability of Pd layers directly deposited on metal supports is hindered by the migration of Pd in the metallic material underneath and vice-versa, a phenomenon known as intermetallic diffusion [16]. This issue can be solved by the deposition of a ceramic layer between Pd and the metallic support, namely as interdiffusion barrier. Several ceramic materials have been investigated as possible interdiffusion barrier layer candidates, such as ZrO_2 [17,18], YSZ [19], Al_2O_3 [20,21], TiO_2 [22], CeO_2 [23,23], zeolites [24,25], siliceous materials [26] or even pencil coatings [27].

Bottino et al. [28] deposited a boehmite layer on stainless steel supports, selecting the ones with most suitable surface characteristics and pore size via bubble point method.

Commercial metallic filters with unrefined surface characteristics prove more economically convenient with respect to the lower media grades commonly used for metallic membrane development, which are scarce on the market. Such unrefined filters can be 8 to 10 times less expensive than pre-treated, low media grade metallic filters rendered suitable for membrane preparation. However, these more economically viable alternatives lack in 1) the surface quality necessary for deposition of a continuous Pd–Ag layer, and in 2) suitable pore size for rendering such layers highly selective (Table 3). This work focuses on tackling the filters' surface roughness improvement issue, in order to achieve deposition of a continuous Pd–Ag layer. Therefore, in this study the interdiffusion barrier layer is employed with a double function: 1) to further reduce the surface roughness of the starting metallic support and 2) to prevent intermetallic diffusion. The deposition via dip-coating of a gamma alumina smoothing interdiffusion layer is presented, starting from a boehmite solution precursor. The layer is deposited on an unrefined Hastelloy X filter, a material which is able to withstand temperatures up to 750°C , allowing for a wide range of possible ceramic sintering conditions and prolonged use at high temperature. The filters are subjected to polishing treatment for variable times, in order to reduce their large average surface roughness and to investigate the effect of pre-treatments on both bare and coated supports. No pre-selection of suitable surface characteristics or pore size of such filters has been carried out: the focus of this work is solely on decreasing the Hastelloy X filters' surface roughness, improving their suitability for Pd–Ag deposition with a universal method. Thus, this work provides a starting point in decreasing the cost of metallic supported Pd–Ag membranes by modifying unrefined porous sintered metallic tubes. Three different polishing times have been evaluated for interdiffusion layer deposition, as well as three ceramic loading percentages for the smoothing interdiffusion layer precursor. Different dip-coating, drying and sintering routes have been assessed aiming for an improvement of support morphology and to allow a successful later Pd–Ag deposition. Supports are characterized in terms of surface roughness via profilometry, N_2 permeance and Scanning electron microscopy (SEM) imaging of the coated layer thickness and surface morphology. A Pd–Ag layer is deposited onto the most suitable support type via electroless plating. The resulting membrane is characterized in terms of ideal hydrogen/nitrogen selectivity and hydrogen permeance.

Experimental

Porous hastelloy X supports

Commercial unrefined porous Hastelloy X filters with an outer diameter of 1.2 cm, average surface roughness (Ra) of 6.1 μm , and 0.5 μm nominal media grade were acquired by Wuhan Shunle stainless steel. The supports are cut in samples of 10 cm length and welded to dense stainless steel (AISI316L) tubes, in order to achieve a one close end configuration. To preliminarily reduce the surface roughness of the filters, the sample supports were polished in an industrial surface finishing machine (ERBA EVT-170) for a time varying between 1 and 12 h, in presence of water. The industrial surface finishing machine delivers polished supports via wet polishing method: the samples are submerged in the polishing media (conical abrasive ceramic chips) in presence of a continuous stream of water. The machine is then able to vibrate for the set amount of time, allowing the polishing media to continuously slide onto and around the samples. The supports are then oxidized for 1 h at 750 °C in a furnace in static air atmosphere, in order to prevent the initial formation of oxides from disrupting the following step of ceramic layer sintering [29]. Before further treatments, the supports are thoroughly rinsed both in ethanol and in deionized water in an ultrasonic bath, in order to remove all impurities resulting from polishing and handling.

Interdiffusion barrier deposition

To deposit the smoothening interdiffusion barrier onto the polished supports, three consecutive steps are carried out: 1) aqueous boehmite-additives dispersion preparation, 2) deposition with controlled immersion speed 3) drying and sintering.

A commercial boehmite solution, namely Alumisol 10 A (Boehmite conc. 10,1 wt%) was acquired from Kawaken Co., Japan. Three sample solutions with boehmite loading 0,9 wt%, 1,2 wt%, 1,8 wt% are prepared by diluting the Alumisol 10 A in distilled water and incorporating it into a water-based solution of organic additives, namely 3.5 wt% polyvinyl alcohol (PVA) (MW 130000) and 1 wt% polyethylene glycol (PEG) (MW 400).

The boehmite dispersion is deposited onto the sample supports via dip-coating with an especially designed automated setup. The setup consists in a pneumatic slider accommodating a membrane holder. The slider can then be programmed remotely according to the parameters listed in Table 1. The selected dip-coating parameters are kept constant for each sample.

Table 1 – Selected dip-coating parameters for interdiffusion layer deposition.

Immersion speed	(mm/s)	5
Withdrawal speed	(mm/s)	5
Waiting time above solution	(s)	10
Waiting time in solution	(s)	5
Number of dips	(–)	2

The deposited layer is dried under rotation in a climate chamber at 40 °C and 60% relative humidity for 1 h. The layer is then sintered for 1 h at 550 °C in a static air furnace.

To compare resulting layer properties, the dip-coating and sintering route for the test supports has been varied, according to Table 2. The number of immersions is the number of times the support is submerged into the boehmite dispersion to form one layer. The number of layers is the amount of dry layers deposited onto each other via drying-dipping-sintering route (DDS) or via sintering-dipping-sintering route (SDS).

Palladium-silver (Pd–Ag) deposition

Prior to plating, the support is seeded with Pd nuclei following the technique described by Tanaka et al. [30], using a chloroform-based Palladium Acetate (II) solution.

A layer of Pd–Ag alloy is deposited onto boehmite coated supports via electroless plating technique, reported in previous work [12]. The plating bath is composed of Palladium acetate (II), AgNO_3 , EDTA, NH_4OH . Hydrazine is added to the plating bath as reducing agent, in presence of the support. A water based AgNO_3 solution is continuously added to the bath with a syringe pump after a base plating of 2 h. The plating procedure was stopped after 5 h. In an effort to close leftover pores, a consecutive plating procedure can be carried out to achieve a thicker layer. Two plating cycles of 5 h each can be performed to achieve a Pd–Ag layer thickness up to 10 μm .

After each plating step, the membrane is annealed at 550 °C in 10 vol% H_2 - 90 vol%Ar atmosphere for 4 h.

Characterizations

Surface roughness and N_2 permeation have been measured in order to assess both polishing effect on the Hastelloy X sample supports, and quality of Al_2O_3 layer after deposition. The surface morphology resulting from polishing treatments is observed via Scanning Electron Microscopy (SEM), as well as the thickness of the deposited interdiffusion barriers and Pd–Ag layers. The samples for imaging are obtained via support scoring and breakage. When observing fully plated membranes, this sample preparation procedure might result in slight detachment of the Pd–Ag layer from the smoothening interdiffusion barrier. However, this technique is employed to preserve the original porous structure of the metallic support, allowing for a thorough observation of the real morphology of the cross section.

The average pore diameter and the largest pore diameter of the untreated Hastelloy X filter were measured via capillary

Table 2 – Sintering-dipping routes used for layer comparison.

Support type	Polishing time	Immersion number	Layers
(–)	(h)	(–)	(–)
Uncoated	6	0	0
S1	6	2	1
S2	6	2	2, SDS
S3	6	2	2, DDS

flow porometry (CFP) technique, with a Porolux 1000 porometer. The sample filter was cut in 1 cm length and sealed to reach a one-close end configuration.

The surface roughness of both the untreated Hastelloy X supports and the one resulting from each polishing time was measured with a portable contact profilometer (MarSurf PS 10) and expressed in terms of nominal average roughness (R_a), average profile height (R_z), maximum peak (R_p) and valley height (R_v). R_a is the absolute value of the arithmetic average of the roughness profile's ordinates. R_z is the arithmetic average of the difference between the highest and lowest points of each profile in the evaluated length. R_p and R_v are the values of the highest and lowest points of the roughness profile, respectively. The roughness parameters are evaluated by averaging the results obtained from 10 random positions on the 10 cm porous support tube.

For uncoated Hastelloy X supports, the permeance of N_2 is evaluated in the permeation setup described in Fig. 1 at 20 °C (room temperature) with a pressure difference of 0,2 bar. The membrane is inserted in a permeation shell, which is connected to N_2 and H_2 feed lines, whose flow is regulated via a mass flow controller. The pressure in the shell is regulated via a manual backpressure regulator at the retentate side. The permeate stream is connected to an automatic bubble flowmeter (Horiba) to measure the outlet gas flow rate. The permeation setup can be heated up to 600 °C, and the temperature is indicated on three different thermocouples placed at various levels in the shell.

For coated supports, N_2 permeance is evaluated at 20 °C (room temperature) with a pressure difference of 1, 2, 4, 6 bar.

After Pd–Ag deposition, the performance of the membrane is evaluated in terms of N_2 permeance at 20 °C with 1 bar pressure difference, as well as H_2/N_2 ideal selectivity at 400 °C.

Results and discussion

Surface characteristics of untreated supports

In order to assess the surface characteristics of the rough tubular filters employed in this work, their average surface roughness, average through pore size and nitrogen permeance at 1 bar, 20 °C are measured before any treatment. These characteristics are compared with the ones of 1) A standard alpha alumina asymmetric support commonly used for thin Pd–Ag membranes preparation, 2) More expensive metallic supports with most commonly used media grades for membrane preparation. It is important to remark that most suppliers of metallic supports do not provide an average pore size, but rather a nominal media grade, which corresponds to the particle size that is rejected in a 95% for a filtration carried out with the support. A lower media grade corresponds to a lower pore size.

Generally, all metallic support types present larger R_a and lower gas permeance compared to the ceramic supports. Physico-chemical treatments operated by the supplier are able to reduce surface roughness and increase gas permeance, but increase support costs. The need for cheaper and more readily available metallic support options leads to the use of 0.5 nominal media grade filters proposed for this work. The larger pore diameter and wide distribution promote gas permeation through widely distributed large pores rather than narrowly distributed nanometer-sized pores of ceramic supports, making it more difficult for the Pd–Ag layer to fully close the superficial pore mouths. Moreover, even though the pores are large, gas permeation is still hindered due to the lower

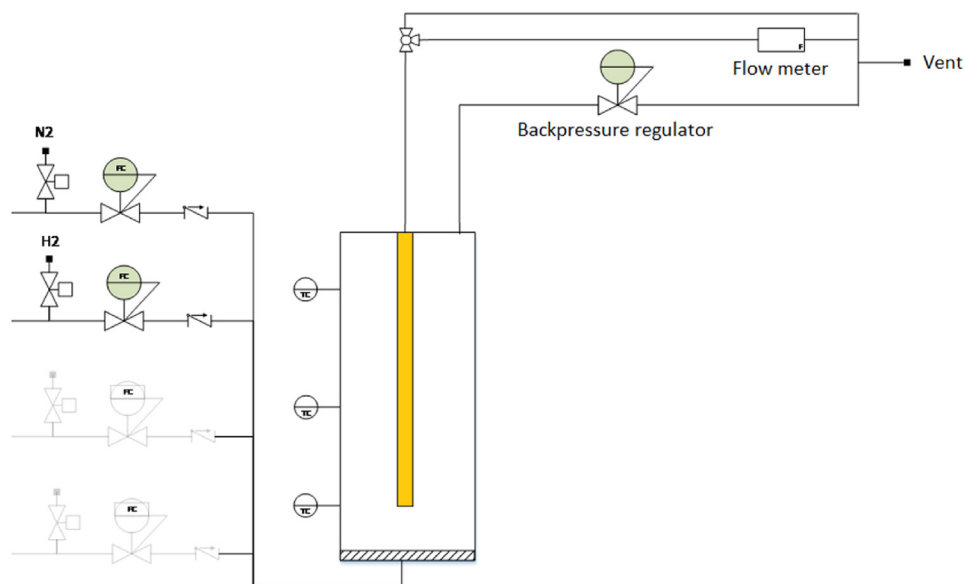


Fig. 1 – Membrane permeation setup.

porosity of the material. A lower Hydrogen permeance through the resulting metallic supported membrane is therefore to be expected with respect to the ceramic relative, regardless of support pre-treatments. Moreover, the surface roughness of the selected filters amounts to $6.1 \mu\text{m}$. A large reduction in surface roughness is therefore crucial for promoting the deposition of thin Pd–Ag layers. For this reason, the wet polishing technique was selected as most suitable candidate for roughness reduction. Moreover, the further addition of a smoothing interdiffusion barrier is proposed in order to push average surface roughness values closer to the ceramic support material and allow for delamination-free Pd–Ag deposition.

3.2 Effect of polishing time on sample filters.

Fig. 2 shows the evolution of both the average height of the roughness profile (Rz) and the average roughness (Ra) of the support with the residence time in the vibratory polishing machine. Increasing the polishing time, both parameters decrease until a plateau is reached around 7 h of polishing. Beyond this time, the variation of both parameters is less significant with respect to shorter polishing time (between 1 and 6 h). Once the plateau is reached, increasing polishing time does not lead to significant changes in average roughness or average profile height. This behavior has been reported in previous works concerning vibratory finishing techniques [32]. In particular, two main mechanisms can be observed for this type of surface treatment: 1) material erosion and 2) plastic deformation. Hashimoto and DeBra measured material removal and surface finish of several workpieces, concluding that material erosion depends on the initial roughness of the workpiece, and it decreases as the roughness of the material decreases [33]. In the work of Baghbanan et al. [34], plastic deformation resulting from media impact and sliding produced curvatures in aluminum alloy workpieces. Fig. 3 shows the evolution of both maximum peak height (Rp) and maximum valley depth (Rv) of the roughness profile of the supports with the residence time in the polishing machine. Rp decreases significantly within the first 2 h of polishing, when the initial roughness of the profile is larger, suggesting erosion of the highest profile points. Rv shows a slower decrease, suggesting valley filling due to plastic deformation from media sliding. At longer polishing times (>7 h), the expected saturation is reached and the change in both parameters becomes less significant.

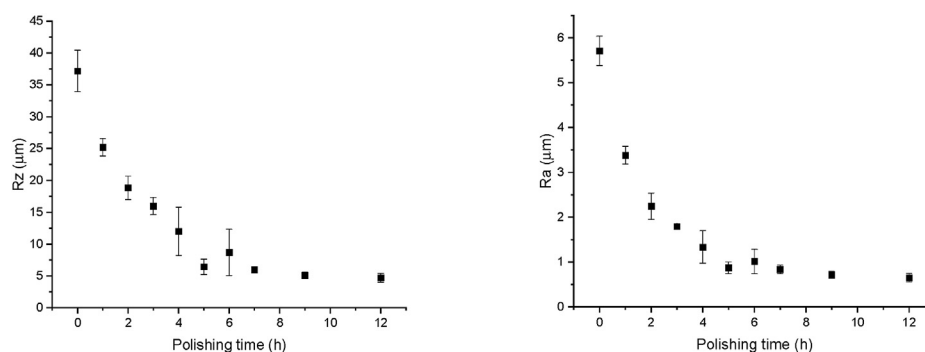


Fig. 2 – Metallic support's average surface roughness (Ra) and average profile height (Rz) evolution with polishing time.

Fig. 4 shows the surface evolution of a support sample with increasing polishing time. In picture 4(a), it is evident the presence of potholes, protuberances, and deep valleys. Pore mouths are as large as $20 \mu\text{m}$. After 3 h of polishing (4(b)) the surface starts to level out. The material removal is confirmed by the presence of scratching on the sample surface, while plastic deformation presents itself with the closure of potholes: part of the surface is pushed tangentially to close the large pore mouths. At this polishing time, however, the shape of the initial structure is still visible. After 6 h of polishing (4(c)) streaks and protuberances are still visible. It is evident the presence of larger streaks, suggesting that plastic deformation is promoting the leveling of the profile peaks. After 9 h (4(d)) the surface is almost fully leveled out, and the initial structure is no longer distinguishable.

In Fig. 5 the nitrogen permeance of supports at each polishing time is reported. The trend shows a decrease of nitrogen permeance with polishing time, suggesting superficial pore closure by plastic deformation of the surface structure [35]. Consequentially, even though smoother supports are the most suitable for Pd–Ag deposition, they will hinder gas permeation through their structure. It is therefore necessary to select the most suitable polishing time for pre-treatment according to the best trade-off between surface roughness reduction and gas permeance preservation.

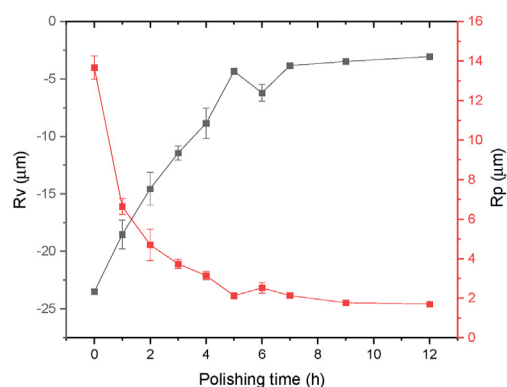


Fig. 3 – Metallic support's maximum peak height (Rp) and maximum valley depth (Rv) evolution with polishing time.

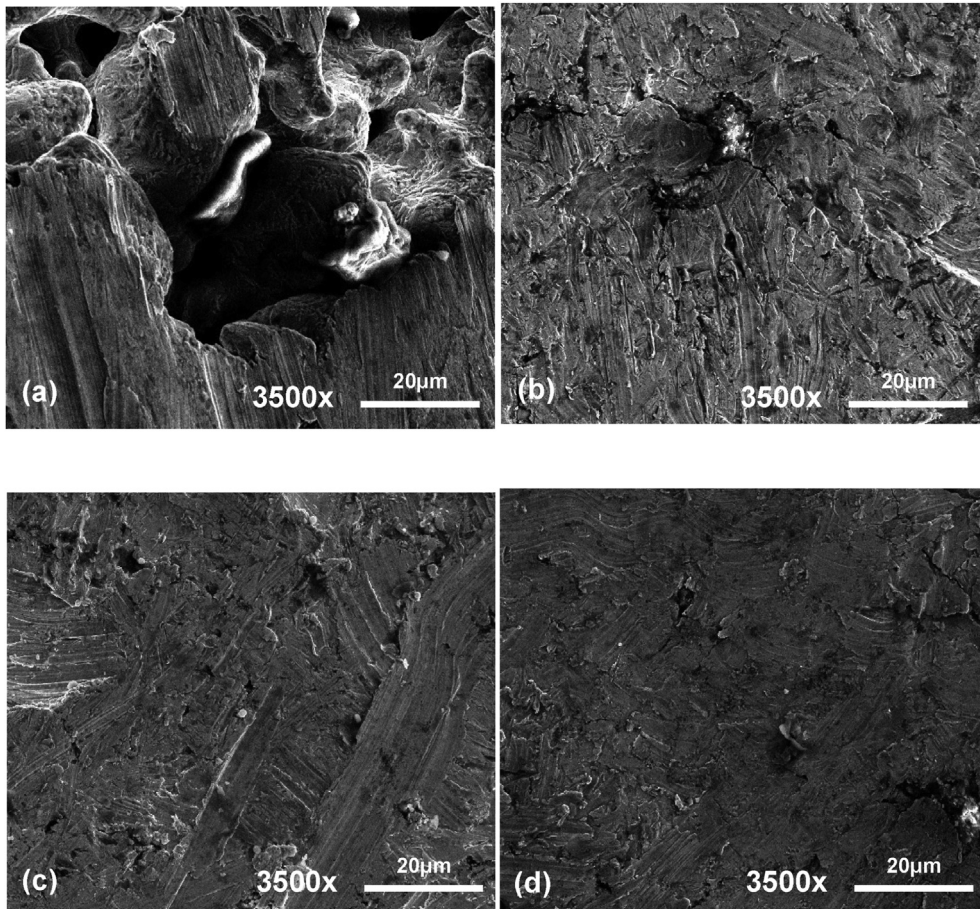


Fig. 4 – SEM imaging of (a) unpolished metallic support surface, (b) surface polished for 3 h, (c) polished for 6 h, and (d) polished for 9 h.

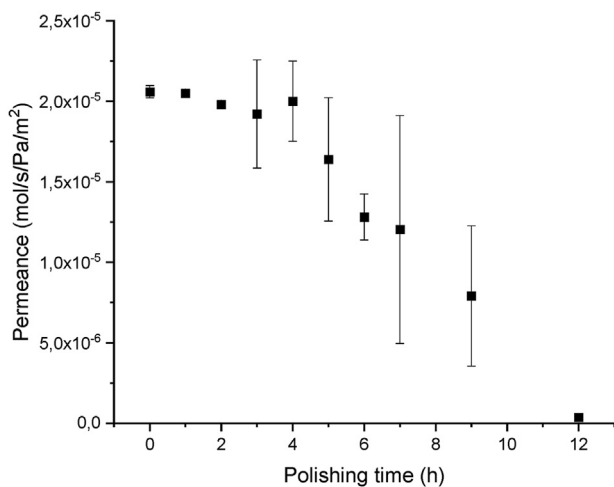


Fig. 5 – N₂ permeance of supports polished at increasing times (20 °C, 0.2 bar).

Physico-chemical characterization of the smoothening interdiffusion barrier

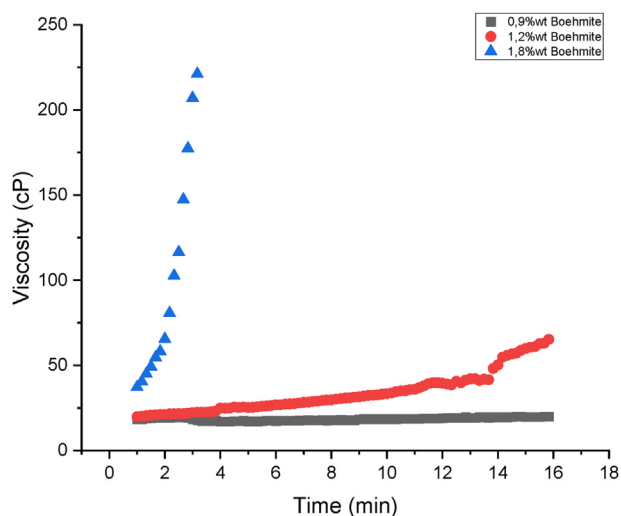
Boehmite solutions are well-known in literature for their pseudoplastic (shear-thinning behavior) at all pH levels,

possibly due to weak forces of attraction between particles (i.e. van der Waals forces) [36]. Moreover, addition of polymers can also influence rheological behavior of the interdiffusion barrier precursors by hampering or enhancing dip-coating, improving or preventing solution stability and reusability, controlling drying stresses, and promoting or hindering coating uniformity after sintering. A crucial point for this work is the dependency of solution viscosity over time, which provides an indication on solution stability and the possibility of storage/reusability. Fig. 6 shows the viscosity evolution with time elapsed from preparation of three sample boehmite solutions, according to their solid loading.

Increasing the amount of boehmite at constant polymers concentration, the dependency of the solution's viscosity on time increases. In particular, the solution prepared with the largest boehmite loading (#sol1, 1,8 wt% boehmite) shows the highest value of viscosity, ranging between 36,6 cp and 222 cp, reaching gelation within 5 min from preparation. Decreasing the solid content (#sol2, 1,2 wt% boehmite), the stability of solution viscosity increases, ranging from 24,5 cp to 9,5 cp within 15 min from preparation at constant shear rate, and reaching gelation behavior within 30 min. A further decrease in solid loading (#sol3, 0,9 wt% boehmite) leads to the lowest viscosity, stable around 18 cp within 15 min from preparation, presenting gelation after a few hours. This behavior suggests

Table 3 – Average surface roughness, pore size and N₂ permeance at 1 bar, RT of commercial porous supports for Pd-based membranes preparation.

Support material (–)	Supplier (–)	Ra (μm)	Average pore size (–)	N ₂ permeance ($\text{mol s}^{-1} \text{m}^{-2} \text{Pa}^{-1}$)	Ref (–)
$\alpha\text{-Al}_2\text{O}_3$	Rauschert	0,58	–100 nm avg. Pore diameter; – narrow pore size distribution	$\sim 8 \cdot 10^{-5}$	[31]
Hastelloy X	Wuhan Shunle SS	6,1	–0.5 μm nominal media grade; –8 μm largest through pore; –1.8 μm mean flow pore	$5 \cdot 10^{-5}$	This work
Hastelloy X, treated	Mott Corp.	0,9	–0.2 μm nominal media grade	$3,54 \cdot 10^{-5}$	[19]
Porous SS	Mott. Corp.	3,2	–0.1 μm nominal media grade	$1,5 \cdot 10^{-5}$	[28]

**Fig. 6 – Viscosity evolution with time of solutions prepared with 0,9 wt%, 1,2 wt%, 1,8 wt% of boehmite with PVA-PEG (3,5 wt% -1wt%) additive.**

that increasing the solid loading at constant additives concentration enhances the non-Newtonian behavior of the solution, showing a rheoplectic (anti-thixotropic) behavior previously reported in literature [37,38].

To achieve uniform interdiffusion layers and increase the support coverage, a trade-off between high boehmite concentration and solution stability with time should be reached. Moreover, to reasonably compare supports performance, solution viscosity must be stable enough to ensure reproducible dip-coating conditions. For this reason, the depositions performed in this work have been carried out with freshly made solutions within 5 min from preparation.

Table 4 shows the average surface roughness (Ra) and the average profile height (Rz) of supports polished for 6 h and coated with the three test solutions. Increasing the boehmite percentage in the precursor solution results in reduced surface roughness of modified supports after sintering, while polishing time is kept constant.

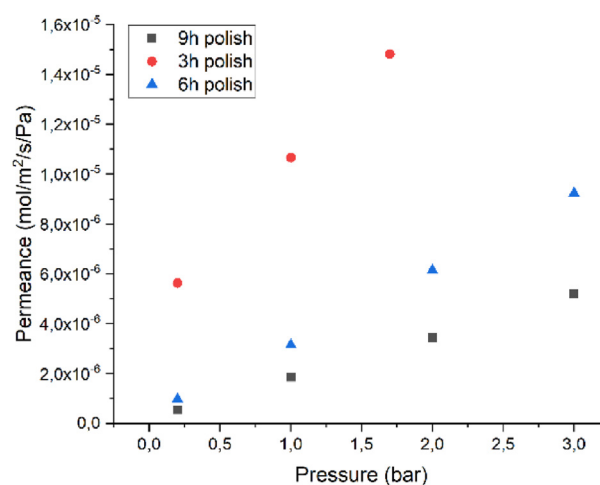
This behavior is reflected by the layer thickness value for each solid loading percentage. As shown in Table 4, increasing the boehmite concentration in the precursor solution leads to an increased layer thickness, due both to the viscosity increase at larger solid load (and thus increased adhesion to the bare support) and to the presence of more solid itself. A

thicker layer promotes support coverage, large pores closure, reduction of average surface roughness and profile height but might act as resistance to gas permeation through the final membrane.

To assess the effect of support polishing time on ceramic layer deposition, a 1,2 wt% boehmite solution was chosen to be deposited on supports polished for 3 h, 6 h and 9 h, respectively. Fig. 7 shows the nitrogen permeance behavior of each modified support. Increasing polishing time, the permeance of the support after deposition decreases. This behavior is to be expected given that a bare support polished

Table 4 – Ra and smoothening layer thickness measured for supports prepared with 0.9 wt%, 1.2 wt% and 1.8 wt% of boehmite loading in the precursor solution.

Support treatment (–)	Ra (μm)	Ra variation (%)	$\gamma\text{-Al}_2\text{O}_3$ Layer thickness (μm)
6h polish, uncoated	0,82	–	–
6h polish, 0,9 wt% boehmite	0,79	3,8	0,54
6h polish, 1,2 wt% boehmite	0,70	14,8	1,1
6h polish, 1,8 wt% boehmite	0,64	21,4	1,8

**Fig. 7 – N₂ permeance measured at 20 °C for supports polished for 3,6,9 h and modified with a precursor solution prepared with 1.2 wt% of boehmite loading.**

for 3 h is more permeable than the others, according to Fig. 5. Depositing the same ceramic precursor on the three selected supports preserves the permeance behavior of the bare supports, resulting in the same decreasing trend.

All supports show positive slope of permeance with pressure in a range from 0 to 3 barg, suggesting the presence of macropores leading to viscous gas flow. The slope reduces with polishing time, indicating a pore closure effect related both to polishing extent and coating introduction. For this reason, studies on coating and polishing influence on pore size modification are in progress.

The initial roughness of a 3 h polished uncoated support is relatively higher compared to the ones polished at longer times (Table 5). For this reason, a large quantity of ceramic coating can be retained by its surface, resulting in a thick layer and a 26,7% reduction in Ra after deposition. Increasing the polishing time to 6 h leads to a

Support rough enough to retain a relatively large amount of ceramic coating, promoting an average roughness reduction of 14,8% and resulting in a uniform layer. The roughness of a 9 h polished uncoated support is relatively lower if compared to the less polished supports. Given a smoother surface, less coating can be retained, resulting in a thinner layer and a reduction of average surface roughness only of 7,1%. Bottino et al. obtained similar behavior by coating porous stainless steel supports rubbed for different times with a pseudo-boehmite precursor solution [28].

Once a bare support polishing time and a base precursor solution composition for the interdiffusion barrier are selected, it is possible to investigate different dip-coating – sintering routes. The main parameters evaluated for this study are 1) the number of immersions of the metallic support into the ceramic precursor solution (namely dips), and 2) the number of smoothening interdiffusion layers deposited on the metallic support. After dipping for a certain amount of times in the precursor solution, each layer can be a) dried only (DDS) or b) dried and sintered (SDS) before a new dipping is performed and a new layer is deposited. Table 6 shows the roughness parameters and the interdiffusion layer thickness evaluation for each selected dipping-sintering route.

The addition of a ceramic precursor layer in S1 reduces average support roughness by 14,8% with respect to a solely polished support. Coverage of the average profile height is promoted, pushing the support's average roughness towards

Table 5 – Ra, Rz and layer thickness measured for supports polished for 3, 6, 9 h and coated with precursor solutions prepared with 1.2 wt% boehmite loading.

Support polishing (h)	Coating composition (boehmite wt%)	Ra (μm)	Ra variation (%)	$\gamma\text{-Al}_2\text{O}_3$ Layer thickness (μm)
3	uncoated	1,64	–	
3	1,2	1,20	26,7	1,16
6	uncoated	0,82	–	
6	1,2	0,70	14,8	1,1
9	uncoated	0,69	–	
9	1,2	0,64	7,1	0,73

Table 6 – Ra, Ra variation and layer thickness measured for supports prepared with different dipping-sintering routes.

Support type, polishing time	Layers, route	Ra (μm)	Ra variation (%)	$\gamma\text{-Al}_2\text{O}_3$ Layer thickness (μm)
(–)	(–)	(μm)	(%)	(μm)
Bare, 6 h	0	0,82	–	
S1, 6 h	1	0,70	14,8	1,1
S2, 6 h	2, SDS	0,61	25,3	2,3
S3, 6 h	2, DDS	0,57	30,6	2

the one of its ceramic relatives. Pd–Ag deposition is already possible for S1, starting from a $\gamma\text{-Al}_2\text{O}_3$ layer 1.1 μm thick. The double sintering route used for S2 leads to a sensible reduction of Ra (25,3% with respect to a solely polished support). The double sintering route leads in fact to an average layer thickness of 2.3 μm , the highest amongst the coating procedures. Such a thick layer, however, can lead to delamination phenomena after sintering. This results in a non-uniformly smoothed profile which is detected by the profilometer. The single sintering route used for S3 is employed in order to be able to achieve a thick layer without promoting delamination after sintering. This route allows in fact the deposition of a second layer while the first one is dry but un-sintered and, therefore, still in its gel form. The two layers are then sintered together at once, avoiding double thermal treatment and minimizing thermal stresses. This results in a larger reduction of average surface roughness, while presenting a thinner layer of 2 μm .

Selection of filter modification route

To be able to deposit a uniform Pd–Ag layer onto the tubular Hastelloy X filters with a universal procedure, the most suitable conditions resulting from the previously listed studies must be selected; namely 1) the most suitable polishing time, 2) the interdiffusion barrier precursor solution's boehmite loading and 3) the dipping-sintering route.

According to, a polishing time of 6 h is close to the maximum possible smoothness given by the wet polishing treatment. Moreover, according to Table 5, at this polishing time the support is still able to retain enough ceramic coating while not excessively hampering the gas permeation (Fig. 7). Considering the lowest roughness/highest permeation possible trade-off, 6 h is chosen as standard polishing time for this work.

According to Fig. 6, an interdiffusion barrier precursor solution prepared with 1,2 wt% of Boehmite is relatively stable within 5 min from preparation. The viscosity increase is not sharp and proceeds relatively slowly, while still providing a flowing viscous solution suitable for dip-coating. The increased viscosity with respect to lower solid loading promotes support coverage and thus surface roughness reduction, while still resulting in a delamination-free layer after sintering (Fig. 8). The amount of 1,2 wt% of boehmite is thus selected as base case solid loading for this work, acting as starting point for further studies on interdiffusion layer optimization.

Table 7 – Comparison of different Pd or Pd–Ag metallic supported membranes obtained via electroless plating technique reported in literature.

Membrane	Selective layer thickness	Metallic support material	Metallic support media grade	Metallic support permeation	Barrier layer	H ₂ permeance	Ideal H ₂ /N ₂ selectivity	Ref.
(material, method)	(μm)	(material, media grade)	(μm)	($\text{mol s}^{-1} \text{m}^{-2} \text{Pa}^{-1}$) $\cdot 10^{-5}$	(material)	($\text{mol s}^{-1} \text{m}^{-2} \text{Pa}^{-1}$) $\cdot 10^{-7}$	(–)	(–)
Pd, PVD-ELP	12	Fe–Cr alloy	–	190	YSZ	4.9	700–10 000	[40]
Pd–Ag, ELP	11	PSS 316 L, 0.2 μm	0.2	–	α -alumina	8.6	3770	[41]
Pd–Ag, ELP	4–5	Hastelloy X, 0.2 μm , pre-treated	0.2	3.54	YSZ, Al ₂ O ₃	10	200 000	[19]
Pd, ELP	20	PSS316L, 0.1 μm	0.1	–	Fe–Cr oxide	4.3	286	[42]
Pd–Ag, ELP	14	PSS316L, 0.1 μm	0.1	1.5	Boehmite precursor, Al ₂ O ₃ based	8	100	[28]
Pd–Ag, ELP	10	Hastelloy X, 0.5 μm , 6 h polish	0.5	1.25	Boehmite precursor, Al ₂ O ₃ based	2	512	This work
Pd-ELP	11	PSS316L, 0.5 μm	0.5	10	Silica based	250	20.7–4.5	[43]

To select a standard dipping-sintering combination, Pd–Ag deposition was performed for each test route mentioned in Table 5. Both S2 and S3 showed non-uniform Pd–Ag deposition due to delamination of the Pd–Ag layer during the plating procedure, due to the excessive smoothing layer thickness given by the two consecutive interdiffusion layers depositions (SDS, DDS routes). Even though it promotes a lower surface roughness reduction, S1 (Fig. 8 (a), (b)) allowed for a uniform Pd–Ag layer to be deposited (Fig. 8 (c), (d)). The single layer results in a lower smoothing interdiffusion barrier thickness, less prone to delamination and less harmful in terms of gas permeance reduction. For this reason, the single layer route is preferred for Pd–Ag deposition.

The strong adhesion between Hastelloy X support and alumina-based layer can be observed in Fig. 8 (a) and 8 (b). The smoothing layer is well-distinguishable and integrated onto the Hastelloy X support's profile, without any delamination present even after the breakage for sample SEM observation preparation. In Fig. 8 (c) and 8 (d), a uniform Pd–Ag layer on a Al₂O₃ based layer resulting from pseudo boehmite deposition onto the Hastelloy X support can be observed. The continuous Pd–Ag layer results from replating onto a support modified with the standardized base procedure. The continuous Pd–Ag layer is well attached to the alumina interdiffusion barrier, while a slight detachment from the Hastelloy X support can be observed, solely to be attributed to the breakage required for SEM imaging. Both the alumina-based layer and the Pd–Ag layer, however, follow the metallic support's profile, without any delamination present in the final membrane. Large partially plated pores can be observed on an otherwise uniformly coated surface. These structures are difficult to close with Pd–Ag deposition and hinder membrane's selectivity. However, the base procedure proved to be able to reduce the bare support surface roughness so that a continuous Pd–Ag layer could be deposited.

A thicker smoothing interdiffusion layer might improve pore closure but provide extra resistance to H₂ permeation and be more prone to delamination either during sintering or seeding procedures. Further studies on interdiffusion barrier optimization are being carried out to improve hydrogen permeability while promoting full surface pores closure.

Membrane testing

The membranes resulting from the previously described standardized base procedure (6 h of polishing, modification with one layer resulting from 1,2 wt% boehmite precursor solution, and double 5 h Pd–Ag deposition) are preliminarily tested for nitrogen permeation at 20 °C and 1 bar. Membrane #1 was chosen for testing at high temperature due to its low value of N₂ permeance at room temperature ($6,2 \cdot 10^{-10} \text{ mol s}^{-1} \text{m}^{-2} \text{Pa}^{-1}$). Fig. 9 (a) shows the hydrogen permeating flux measured between 350 °C and 500 °C. Hydrogen permeation increases both with transmembrane pressure increase and temperature increase, showing linear behavior for the pressure exponential factor $n = 0,6$. This exponent deviates from the one often observed with Sievert's law ($n = 0,5$) for ceramic supported membranes at low pressure, indicating a contribution of the metallic support and/or the interdiffusion layer to gas transport through the membrane. This behavior has been previously

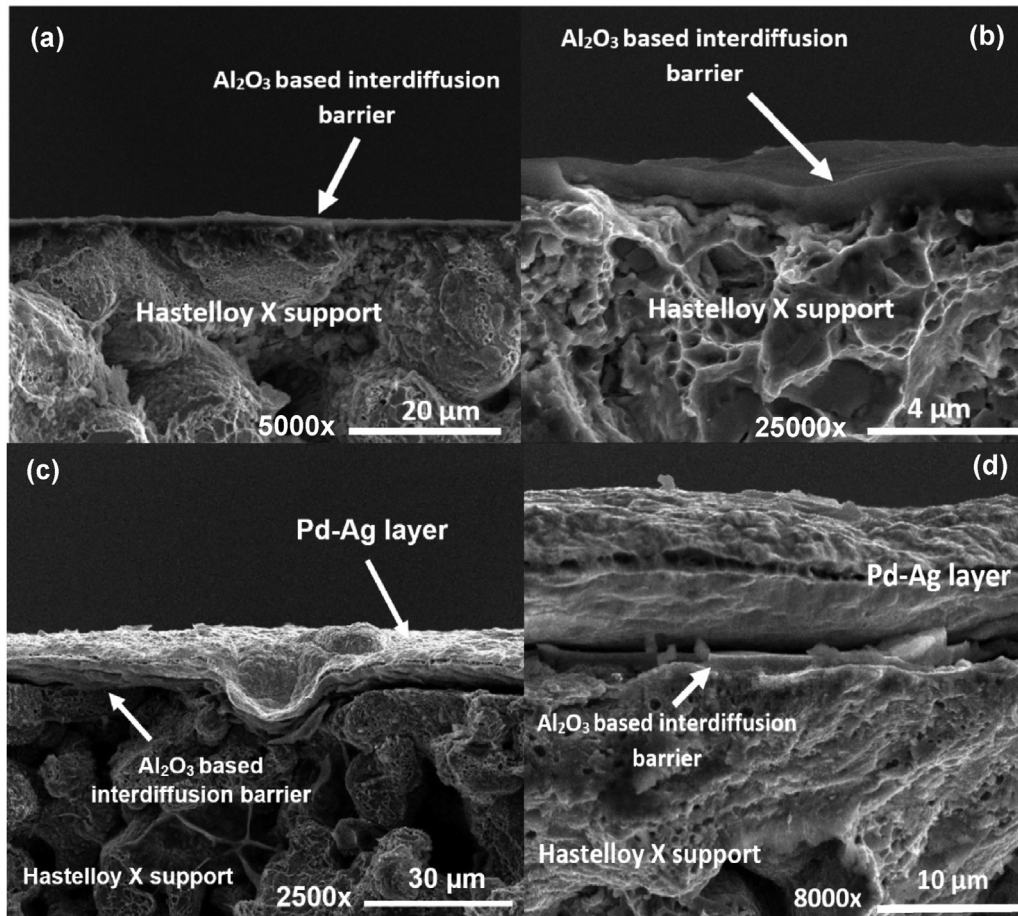


Fig. 8 – Cross sectional SEM images of a well-attached γ - Al_2O_3 smoothing interdiffusion barrier on a Hastelloy X filter, obtained from a 1,2 wt% boehmite-based precursor solution at (a) 5000x, (b) 25000x. A Pd–Ag continuous layer deposited on a tubular Hastelloy X filter modified with a 1,2 wt% of boehmite-based solution at (c) 2500x, (d) 8000x.

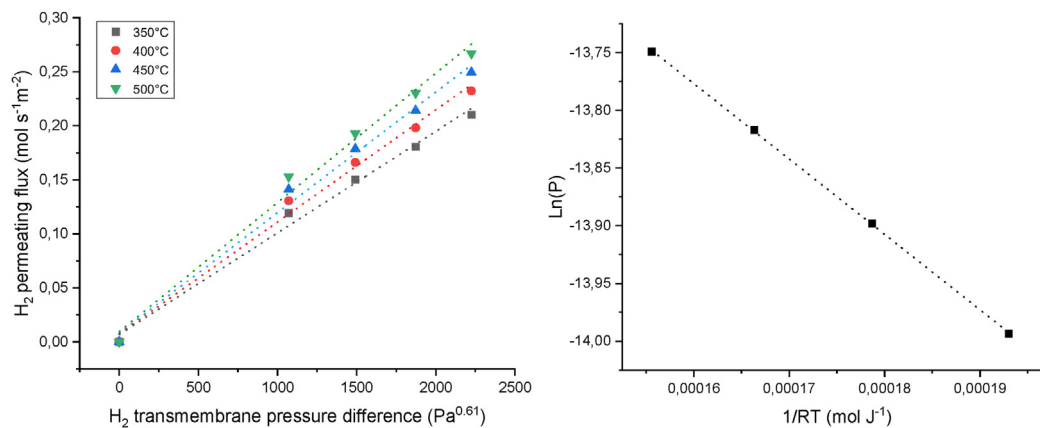


Fig. 9 – (a) H_2 permeating flux vs H_2 partial pressure at different temperatures of membrane #1 (Hastelloy X polished for 6 h, 1.2 wt% boehmite based precursor solution for Al_2O_3 based interdiffusion layer and double 5 h plating of Pd–Ag), (b) linear regression performed on Arrhenius plot to determine membrane's activation energy as slope (ΔE_a , in $\text{kJ}\cdot\text{mol}^{-1}$) and pre-exponential factor as intercept (P_0 , in $\text{mol s}^{-1} \text{m}^{-2} \text{Pa}^{-1}$).

observed in literature for metallic supported membranes [28,39].

The membrane's parameters have been retrieved via the Arrhenius plot of the logarithm of membrane's permeance

(evaluated with 1 bar transmembrane pressure) versus the reciprocal of the temperature (Fig. 9b). The regressed parameters correspond to a maximized $R^2 = 0,992$: activation energy $\Delta E_a = 6,53 \text{ kJ mol}^{-1}$ and pre-exponential factor

$P_0 = 2,96 \cdot 10^{-6} \text{ mol s}^{-1} \text{ m}^{-2} \text{ Pa}^{-0.5}$, both similar to values previously reported in literature for membranes of this kind [39].

Table 7 compares membrane #1 with other literature works on metallic supported Pd–Ag membranes obtained via electroless plating techniques.

At 400 °C, membrane #1 shows a N_2 permeance of $3,7 \cdot 10^{-10} \text{ mol s}^{-1} \text{ m}^{-2} \text{ Pa}^{-1}$. Increasing the transmembrane pressure, N_2 permeance increases with a positive slope. This trend suggests the presence of uncovered pores on the final membrane that result in viscous flow of N_2 . The presence of partially closed pores was further confirmed by both SEM imaging of membrane's surface and a helium leak test in ethanol, which highlighted the presence of a bubble flow from a few scattered pores. Membrane #1 was obtained by Pd–Ag deposition on a 0.5 μm media grade filter, one of the largest media grades to be used as membrane support. For this reason, even though the surface roughness is successfully reduced and Pd–Ag deposition achieved, the large pores of the support do not achieve full closure. Therefore, further studies on filter pre-treatments optimization are in progress, with a focus on narrowing their pore size distribution. The membrane's H_2 permeance at 400 °C amounts to $2 \cdot 10^{-07} \text{ mol s}^{-1} \text{ m}^{-2} \text{ Pa}^{-1}$. This low value might be reconducted to the resistance to gas flow caused by the introduction of a thicker, smoothing interdiffusion layer, as well as the closure effect promoted by polishing on the bare metallic filter, which leads to a less permeable support. These steps, however, prove crucially necessary in order to reduce the filter's roughness and allow the deposition of Pd–Ag. Filters surface roughness reduction must in fact be promoted along with intermetallic diffusion prevention, requiring thicker ceramic layers to promote uniform Pd–Ag deposition.

Conclusions

Deposition of a continuous selective Pd–Ag layer can be achieved via surface modification of rough Hastelloy X filters and introduction of an alumina-based smoothing interdiffusion barrier. The surface of the Hastelloy tube can be pre-treated via wet vibratory finishing technique, leading to both material removal and plastic deformation from media action. The most suitable polishing time for a preliminary preparation procedure is selected as 6 h, as it promotes enough roughness reduction and prevents excessive gas permeation reduction. Moreover, increasing bare support's polishing time leads to less coating retention, thinner layers, and less average surface roughness reduction with respect to supports polished for shorter amounts of time.

The support can be further modified by introduction of a continuous, delamination-free alumina-based smoothing interdiffusion layer, starting from a boehmite dispersion. The composition of the dispersion (both in terms of additive concentration and solid load) influences its rheological properties, which eventually affects smoothing interdiffusion layer thickness, continuity and coverage effect. Storage and reuse of boehmite based dispersions proves difficult due to their anti-thixotropic nature and gelation as early as 5 min from preparation for the highest solid concentration. Increasing the

solution's boehmite loading leads to increased layer thickness and support's average surface reduction. 1,2 wt% of boehmite in the dispersion is selected as trade-off between stability and sufficient support coverage. Depositing and sintering more than one smoothing interdiffusion layer leads to delamination either after ceramic layer sintering or after Pd–Ag deposition, due to excessive layer thickness. Membranes obtained from filters modified with the standardized procedure show the presence of partially covered pore mouths, resulting in partially open pores on the Pd–Ag layer, hindering selectivity. Moreover, the membranes exhibit low hydrogen permeance, which could be attributed to the resistance promoted by the smoothing interdiffusion barrier and the closure effect promoted by polishing. However, these pre-treatments prove themselves crucial for surface roughness improvement. Overall, boehmite based dispersions prove themselves as valuable candidates for smoothing interdiffusion layers, due to their adhesive/binding properties and ability to noticeably reduce the filter's surface roughness. Surface roughness reduction of the unrefined Hastelloy X filters proved possible, opening to the possibility of more economically viable options for supports selection. Future works will focus on filter's superficial pore size optimization, in order to both reduce defect size and increase porosity. Tuning filter pre-treatments proves in fact crucial in order to increase final membrane's H_2 permeance and, consequently, H_2 selectivity.

Declaration of competing interest

The authors declare that they have no known competing financial interests or personal relationships that could have appeared to influence the work reported in this paper.

Acknowledgements



This project has received funding from the European Union's Horizon 2020 Research and Innovation Programme under grant agreement No 869896 (MACBETH).

REFERENCES

- [1] Gallucci F, Fernandez E, Corengia P, van Sint Annaland M. Recent advances on membranes and membrane reactors for hydrogen production. *Chem Eng Sci* 2013;92:40–66. <https://doi.org/10.1016/j.ces.2013.01.008>.
- [2] Bernardo G, Araújo T, da Silva Lopes T, Sousa J, Mendes A. Recent advances in membrane technologies for hydrogen purification. *Int J Hydrogen Energy* Mar. 2020;45(12):7313–38. <https://doi.org/10.1016/j.ijhydene.2019.06.162>.
- [3] Fernandez E, et al. Palladium based membranes and membrane reactors for hydrogen production and purification: an overview of research activities at Tecnalia

- and TU/e. *Int J Hydrogen Energy* 2017;42(19):13763–76. <https://doi.org/10.1016/j.ijhydene.2017.03.067>.
- [4] Park J, Bennett T, Schwarzmann J, Cohen SA. Permeation of hydrogen through palladium. *J Nucl Mater* 1995;220–222(2):827–31. [https://doi.org/10.1016/0022-3115\(94\)00591-5](https://doi.org/10.1016/0022-3115(94)00591-5).
- [5] Alique D, Martinez-Diaz D, Sanz R, Calles JA. Review of supported Pd-based membranes preparation by electroless plating for ultra-pure hydrogen production 2018;8(1).
- [6] Gallucci F, Paturzo L, Basile A. A simulation study of the steam reforming of methane in a dense tubular membrane reactor. *Int J Hydrogen Energy* 2004;29(6):611–7. <https://doi.org/10.1016/j.ijhydene.2003.08.003>.
- [7] Patil CS, van Sint Annaland M, Kuipers JAM. Fluidised bed membrane reactor for ultrapure hydrogen production via methane steam reforming: experimental demonstration and model validation. *Chem Eng Sci* 2007;62(11):2989–3007. <https://doi.org/10.1016/j.ces.2007.02.022>.
- [8] Bernardo P, Barbieri G, Drioli E. Evaluation of membrane reactor with hydrogen-selective membrane in methane steam reforming. *Chem Eng Sci* Feb. 2010;65(3):1159–66. <https://doi.org/10.1016/j.ces.2009.09.071>.
- [9] Arratibel Plazaola A, Pacheco Tanaka DA, Van Sint Annaland M, Gallucci F. Recent advances in Pd-based membranes for membrane reactors. *Molecules* 2017;22(1). <https://doi.org/10.3390/molecules22010051>.
- [10] Arratibel A, Pacheco Tanaka DA, Slater TJA, Burnett TL, van Sint Annaland M, Gallucci F. Unravelling the transport mechanism of pore-filled membranes for hydrogen separation. *Separ Purif Technol* 2018;203(April):41–7. <https://doi.org/10.1016/j.seppur.2018.04.016>.
- [11] Arratibel A, Pacheco Tanaka A, Laso I, van Sint Annaland M, Gallucci F. Development of Pd-based double-skinned membranes for hydrogen production in fluidized bed membrane reactors. *J Membr Sci* 2018;550:536–44. <https://doi.org/10.1016/j.memsci.2017.10.064>. August 2017.
- [12] Pacheco Tanaka DA, et al. Preparation of palladium and silver alloy membrane on a porous α -alumina tube via simultaneous electroless plating. *J Membr Sci* 2005;247(1–2):21–7. <https://doi.org/10.1016/j.memsci.2004.06.002>.
- [13] de Nooijer N, et al. Long-term stability of thin-film Pd-based supported membranes. *Processes* 2019;7:2. <https://doi.org/10.3390/pr7020106>.
- [14] Fernandez E, et al. Development of thin Pd–Ag supported membranes for fluidized bed membrane reactors including WGS related gases. *Int J Hydrogen Energy* 2015;40(8):3506–3519, Mar. <https://doi.org/10.1016/j.ijhydene.2014.08.074>.
- [15] Mardilovich IP, Engwall E, Ma YH. Dependence of hydrogen flux on the pore size and plating surface topology of asymmetric Pd-porous stainless steel membranes. *Desalination Sep.* 2002;144(1–3):85–9. [https://doi.org/10.1016/S0011-9164\(02\)00293-X](https://doi.org/10.1016/S0011-9164(02)00293-X).
- [16] Van Dal MJH, Pleumeekers MCLP, Kodentsov AA, Van Loo FJJ. Intrinsic diffusion and Kirkendall effect in Ni–Pd and Fe–Pd solid solutions. *Acta Mater Jan.* 2000;48(2):385–96. [https://doi.org/10.1016/S1359-6454\(99\)00375-4](https://doi.org/10.1016/S1359-6454(99)00375-4).
- [17] Tarditi A, Gerboni C, Cornaglia L. PdAu membranes supported on top of vacuum-assisted ZrO₂-modified porous stainless steel substrates. *J Membr Sci Feb.* 2013;428:1–10. <https://doi.org/10.1016/j.memsci.2012.10.029>.
- [18] Contardi I, Cornaglia L, Tarditi AM. ScienceDirect Effect of the porous stainless steel substrate shape on the ZrO₂ deposition by vacuum assisted dip-coating. *Int J Hydrogen Energy* 2017;42(12):7986–96. <https://doi.org/10.1016/j.ijhydene.2017.01.024>.
- [19] Fernandez E, et al. Preparation and characterization of metallic supported thin Pd–Ag membranes for hydrogen separation. *Chem Eng J* 2016;305:182–90. <https://doi.org/10.1016/j.cej.2015.09.119>.
- [20] Bosko ML, Miller JB, Lombardo EA, Gellman AJ, Cornaglia LM. Surface characterization of Pd–Ag composite membranes after annealing at various temperatures. *J Membr Sci Mar.* 2011;369(1–2):267–76. <https://doi.org/10.1016/j.memsci.2010.12.006>.
- [21] Xu N, Ryi S, Li A, Grace JR, Lim J, Boyd T. Improved pre-treatment of porous stainless steel substrate for preparation of Pd-based composite membrane. *Can J Chem Eng* 2013;91(10):1695–701. <https://doi.org/10.1002/cjce.21793>.
- [22] Straczewski G, et al. Development of thin palladium membranes supported on large porous 310L tubes for a steam reformer operated with gas-to-liquid fuel. *Chem Eng Process Process Intensif Jul.* 2014;81:13–23. <https://doi.org/10.1016/j.cep.2014.04.002>.
- [23] Qiao A, et al. Hydrogen separation through palladium–copper membranes on porous stainless steel with sol–gel derived ceria as diffusion barrier. *Fuel* 2010;89(6):1274–1279, Jun. <https://doi.org/10.1016/j.fuel.2009.12.006>.
- [24] Bosko ML, Múnera JF, Lombardo EA, Cornaglia LM. Dry reforming of methane in membrane reactors using Pd and Pd–Ag composite membranes on a NaA zeolite modified porous stainless steel support. *J Membr Sci Nov.* 2010;364(1–2):17–26. <https://doi.org/10.1016/j.memsci.2010.07.039>.
- [25] Kiadehi AD, Taghizadeh M. ScienceDirect Fabrication , characterization , and application of palladium composite membrane on porous stainless steel substrate with NaY zeolite as an intermediate layer for hydrogen purification. *Int J Hydrogen Energy* 2018;44(5):2889–904. <https://doi.org/10.1016/j.ijhydene.2018.12.058>.
- [26] Calles JA, Sanz R, Alique D. Influence of the type of siliceous material used as intermediate layer in the preparation of hydrogen selective palladium composite membranes over a porous stainless steel support. *Int J Hydrogen Energy* 2012;37(7):6030–42. <https://doi.org/10.1016/j.ijhydene.2011.12.164>.
- [27] Wei L, Yu J, Hu X, Huang Y. Fabrication of H₂ -permeable palladium membranes based on pencil-coated porous stainless steel substrate. *Int J Hydrogen Energy* 2012;37(17):13007–12. <https://doi.org/10.1016/j.ijhydene.2012.05.064>.
- [28] Bottino A, et al. Sol-gel synthesis of thin alumina layers on porous stainless steel supports for high temperature palladium membranes. *Int J Hydrogen Energy* 2014;39(9):4717–24. <https://doi.org/10.1016/j.ijhydene.2013.11.096>.
- [29] Molin S, Dunst KJ, Karczewski J, Jasiński P. High temperature corrosion evaluation of porous Hastelloy X alloy in air and humidified hydrogen atmospheres. *J Electrochem Soc* 2016;163(6):C296–302. <https://doi.org/10.1149/2.0741606jes>.
- [30] Pacheco Tanaka DA, Llosa Tanco MA, Okazaki J, Wakui Y, Mizukami F, Suzuki TM. Preparation of ‘pore-fill’ type Pd–YSZ– γ -Al₂O₃ composite membrane supported on α -Al₂O₃ tube for hydrogen separation. *J Membr Sci* 2008;320(1–2):436–41. <https://doi.org/10.1016/j.memsci.2008.04.044>.
- [31] Melendez J, Fernandez E, Gallucci F, van Sint Annaland M, Arias PL, Pacheco Tanaka DA. Preparation and characterization of ceramic supported ultra-thin (~1 μ m) Pd–Ag membranes. *J Membr Sci* 2017;528:12–23. <https://doi.org/10.1016/j.memsci.2017.01.011>. 2017.
- [32] Prakasam PK, Castagne S, Subbiah S. Mechanism of surface evolution in vibratory media finishing. *Procedia Manuf* 2015;1:628–36. <https://doi.org/10.1016/j.promfg.2015.09.052>.

- [33] Hashimoto F, DeBra DB. Modelling and optimization of vibratory finishing process. *CIRP Ann Jan.* 1996;45(1):303–6. [https://doi.org/10.1016/S0007-8506\(07\)63068-6](https://doi.org/10.1016/S0007-8506(07)63068-6).
- [34] Baghbanan MR, Yabuki A, Timsit RS, Spelt JK. Tribological behavior of aluminum alloys in a vibratory finishing process. *Wear* 2003;255(7–12):1369–1379, Aug. [https://doi.org/10.1016/S0043-1648\(03\)00124-8](https://doi.org/10.1016/S0043-1648(03)00124-8).
- [35] Iquebal AS, Sagapuram D, Bukkapatnam STS. Surface plastic flow in polishing of rough surfaces. *Sci Rep* 2019;9(1):1–12. <https://doi.org/10.1038/s41598-019-46997-w>.
- [36] Islam MA, Ming CC, Ravindra P, Chen ES. Rheology and gelling behavior of boehmite sols. *J Appl Sci* 2011;11(13):2327–33. <https://doi.org/10.3923/jas.2011.2327.2333>.
- [37] Naskar MK, Chatterjee M, Ganguli D. Rheological properties of boehmite sols during ageing at room temperature ($30 \pm 1^\circ\text{C}$) under closed condition. *Bull Mater Sci* 2002;25(2):115–9. <https://doi.org/10.1007/BF02706230>.
- [38] Çetinel AF, Simon RA. Nanoparticle assisted coagulation of aqueous alumina suspensions. *Mater Res* 2012;15(1):81–9. <https://doi.org/10.1590/S1516-14392011005000091>.
- [39] Preparation and characterization of [1] E. Fernandez et al., Fernandez E, et al. Preparation and characterization of metallic supported thin Pd–Ag membranes for hydrogen separation. *Chem Eng J* 2016;305:182–90. <https://doi.org/10.1016/j.cej.2015.09.119>. metallic support,” *Chem. Eng. J.*, vol. 305, pp. 182–190, 2016, doi: 10.1016/j.cej.2015.09.119.
- [40] Dittmar B, et al. Methane steam reforming operation and thermal stability of new porous metal supported tubular palladium composite membranes. *Int J Hydrogen Energy* 2013;38(21):8759–71. <https://doi.org/10.1016/j.ijhydene.2013.05.030>.
- [41] Augustine AS, Mardilovich IP, Kazantzis NK, Hua Ma Y. Durability of PSS-supported Pd-membranes under mixed gas and water-gas shift conditions. *J Membr Sci* 2012;415–416:213–20. <https://doi.org/10.1016/j.memsci.2012.05.001>.
- [42] Liguori S, et al. Performance of a Pd/PSS membrane reactor to produce high purity hydrogen via WGS reaction. *Catal Today* 2012;193(1):87–94. <https://doi.org/10.1016/j.cattod.2012.02.005>.
- [43] Katoh M, Ueshima T, Takatani M, Sugiura H, Ominami K, Sugiyama S. Effects of different silica intermediate layers for hydrogen diffusion enhancement of palladium membranes applied to porous stainless steel support. *Sci Rep* 2020;10(1):1–12. <https://doi.org/10.1038/s41598-020-62054-3>.